Photonic-Crystal-Fiber-Coupled, Hand-Held, Polarization-Resolved Second-Harmonic-Generation Microscope for *In Vivo* Visualization of Dermal Collagen Fibers in Human Skin

Yuki Ogura, Kosuke Atsuta, Eiji Hase, Takeo Minamikawa, and Takeshi Yasui

***Abstract*—Second-harmonic-generation (SHG) microscopy is a powerful tool for *in vivo* monitoring of collagen fibers in human skin. Furthermore, polarization-resolved SHG microscopy can provide additional insights regarding the direction of collagen fibers, i.e., collagen fiber orientation. However, their practical use in the dermatological field is still limited due to the bulky and complicated setup. In this paper, we constructed a photonic-crystal-fiber (PCF) coupled, hand-held polarization-resolved SHG microscope for *in vivo* monitoring of collagen fibers in human skin. Fiber delivery of ultrashort pulse light was achieved without significant change of the linear polarization by a large-mode-area PCF, whereas the SHG microscopy setup was enclosed into a hand-held probe head. The combination of PCF with the hand-held probe head largely enhances the flexibility of measurement sites in the human skin.**

***Index Terms*—Optical microscopy, optical harmonic generation, biophotonics, biomedical optical imaging.**

I. Introduction

SECOND-HARMONIC-GENERATION microscopy (SHG-M) is an interesting new tool for observing collagen fiber in biological tissues [1]. SHG-M provides unique imaging characteristics: high image contrast, high spatial resolution, optical three-dimensional (3D) sectioning, low invasiveness, deep penetration, and no interference from background light. More importantly, by using the naturally endogenous SHG process as a contrast mechanism, the structure of collagen fibers in tissue can be clearly visualized *in vivo* without additional staining. For example, SHG-M equipped with a 800-nm mode-locked Ti:Sapphire laser has been used for selective visualization of collagen fibers in skin [2], [3], cornea [4], bone [5], cartilage [6], tendon [7], and cultured cell model [8]. Furthermore, combination of SHG-M and polarimetry, namely polarization-resolved SHG-M or PR-SHG-M, can provide additional insights regarding the direction of collagen fibers, i.e., collagen fiber orientation [9]–[12]. This is because the efficiency of SHG light is sensitive to collagen fiber orientation when the incident light is linearly polarized: strong SHG light for parallel configuration and weak SHG light for perpendicular configuration. In spite of such high functionality, the clinical use of SHG-M or PR-SHG-M is still restricted.

One reason for this restriction is in the bulky, complicated, fixed SHG-M setup. From the viewpoint of patent's burden reduction in clinical applications, characteristics of compactness, convenience, robustness, maintenance-free, and flexibility are required in SHG-M. To meet these requirements, (a) miniaturization of SHG-M probe, (b) miniaturization of laser source, and (c) transmission of laser light via optical fiber are important technical elements. Since commercialized compact optics and mechanical components can be used for packing optical components into a hand-held probe, a hand-held SHG-M probe was constructed by use of custom design lens and 3D microscanner [13]. However, use of the mode-locked Ti:Sapphire laser conflicts with a compact and simple SHG-M. Furthermore, although the ultrashort pulse laser light could be delivered to the hand-held SHG-M probe by a 2.5-m double clad fiber (DCF), use of such long DCF needs the bulky external dispersion compensator (grating pair) to avoid the pulse broadening caused by the DCF. Recently, a 1030-nm mode-locked Yb-fiber laser, in place of the mode-locked Ti:Sapphire laser, has been used for the hand-held SHG-M probe [14]. Such all-fiber SHG-M benefits from cost effectiveness, fiber optics flexibility, and compactness; howver, the external dispersion compensator was still needed. Although very low risk of thermal or photochemical damage of the tissue is another advantage of SHG-M at this wavelength band, use of the longer-wavelength laser light is favorable to further suppress the damage.

The wavelength within the range from 1200 to 1300 nm is the best for optical window in biological tissues because of the decreased scattering and absorption in tissues. A promising laser

Manuscript received April 4, 2018; revised July 26, 2018 and August 13, 2018; accepted August 13, 2018. Date of publication August 17, 2018; date of current version September 17, 2018. *(Corresponding author: Takeshi Yasui.)*

Y. Ogura is with the Graduate School of Advanced Technology and Science, Tokushima University, Tokushima 770-8506, Japan (e-mail: yuki.ogura1@to.shiseido.co.jp).

K. Atsuta and E. Hase were with the Graduate School of Advanced Technology and Science, Tokushima University, Tokushima 770-8506, Japan (e-mail: truth0f.telecaster.ash@gmail.com; hase@spring8.or.jp).

T. Minamikawa and T. Yasui are with the Graduate School of Technology, Industrial and Social Sciences, Tokushima University, Tokushima 770-8506, Japan (e-mail: minamikawa.takeo@tokushima-u.ac.jp; yasui.takeshi@tokushima-u.ac.jp).

Color versions of one or more of the figures in this paper are available online at http://ieeexplore.ieee.org.

Digital Object Identifier 10.1109/JSTQE.2018.2865779

source for this wavelength light is a mode-locked Cr:Forsterite laser centered around 1250 nm; it has emerged as a new source for SHG-M, showing decreased photodamage [15]–[17] and enhanced penetration depth [18]. Thanks to these benefits, the 1250 nm-band SHG-M or PR-SHG-M has been used in dermatological applications *in vivo* or *ex vivo*, such as skin aging [19], skin burn [20], skin burn healing [21], skin wound healing [22], and skin wrinkling [23], [24].

Since the state-of-art large-mode-area photonic crystal fiber (LMA-PCF) technology [25] enables us to deliver the femtosecond pulse light without the need for external dispersion compensators, it was used for delivering of the Cr:Forsterite laser light to the hand-held SHG-M probe [26], [27]. The 80-fs pulse light could be delivered with little pulse broadening by a 75-cm LMA-PCF even though no external dispersion compensator was used [27]. However, there are no attempts to expand it to PR-SHG-M.

In this paper, we modified our previous fiber-coupled, hand-held SHG-M [27] for PR-SHG-M and evaluated its performance. We demonstrated *in vivo* visualization of collagen fiber in human skin.

II. Materials and Methods

A. Experimental Setup

Figure 1(a) shows the experimental setup of the hand-held PR-SHG-M. A mode-locked Cr:Forsterite laser (Cr:F-L; Avesta Project Ltd., CrF-65P, center wavelength = 1250 nm, pulse duration = 80 fs, mean power = 250 mW, repetition rate = 73 MHz) pumped by a 1064-nm Ytterbium fiber laser was used as a laser source. We used a LMA-PCF (Thorlabs, Inc., LMA-25, core diameter = 25 μm, NA = 0.05, length = 75 cm) for fiber-delivery of the laser light. In this LMA-PCF, mode dispersion and wavelength dispersion are largely reduced by the designed PCF structure. Furthermore, the large mode-area diameter suppresses unnecessary optical nonlinear effects in the fiber and hence the pulse distortion. After passing through a polarizer (P) and a half-waveplate (λ/2) for linear polarization and its rotation, the laser light was incident into the LMA-PCF with a coupling efficiency of 33% by use of an objective lens (Edmund Optics, magnification = 4, NA = 0.10). We did not observe any long-term thermal or other damages to the LMA-PCF input end. The matching of NA between the LMA-PCF and the objective lens will further improve the coupling efficiency. The laser light propagated in the LMA-PCF and then were fed into a hand-held SHG-M probe. The SHG-M was composed of a fiber collimator, a pair of galvano-mirrors (GM), relay lenses (RL1 and RL2), a harmonic separator (HS; reflected wavelength = 625 nm), an objective lens (OL; Nikon Instruments Inc., CFI Plan 50 × H, magnification = 50, NA = 0.9, working distance = 350 μm, oil-immersion type), an optical band-pass filter (BPF; transmitted wavelength = 625 nm), and a photon-counting photomultiplier (PMT; Hamamatsu Photonics K. K., H7155-01). After passing through the fiber collimator, GM, RL1, RL2, and HS, the laser beam was focused onto the sample with the OL. The SHG light back-scattered from the sample was reflected by HS, is filtered by the BPF, and then was detected by PMT. While the focus of the laser light was two-dimensionally scanned over the sample by GM, it was scanned along the depth direction by a translation stage. These optical systems were enclosed in the lens tube system (Thorlabs, Inc.) [see Fig. 1(b)]. For comparison, Fig. 1(c) shows an optical photograph of our previous SHG-M [19]. Since volume of this hand-held SHG-M

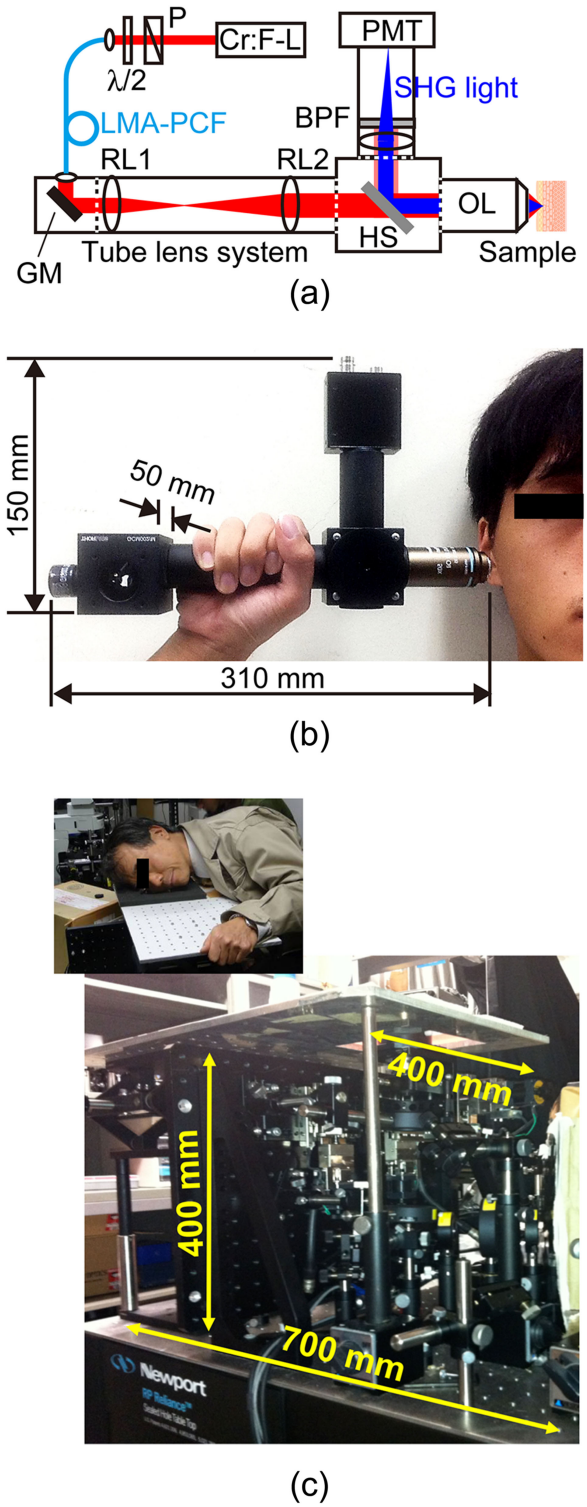

Fig. 1. (a) Schematic diagram and (b) optical photograph of hand-held PR-SHG-M. (c) Optical photograph of conventional SHG-M.

probe (310 mm wide, 150 mm height, and 50 mm depth) was only 5% of that of our previous SHG-M (700 mm wide, 400 mm height, and 400 mm depth), one can hold it by hand as shown in Fig. 1(b).

B. In Vivo Measurement of Human Skin

To evaluate the risk of photodamage to human skin, we previously examined changes in the subjects' skin before, immediately after, and one month after irradiation with a laser light, based on color measurement with a spectrophotometer (Konica Minolta, CM-2600d) and clinical evaluation by a board-certified dermatologist [19]. We concluded from these examinations that there was no laser-induced photodamage to the skin under irradiation of 35-mW laser light, corresponding to the damage threshold of 6.2 MW/cm^2. Based on this evidence, we set the average power of the laser light radiated onto the skin to 30 mW. Written informed consent was obtained from the subject before the measurement. The protocol conformed to the Helsinki Declaration and was approved by the ethics committee for human experiment in Tokushima University (No. 14003). We measured the SHG image of collagen fiber at the cheek skin in the 20's male subject.

III. Results and Discussion

A. Fiber Delivery of Linearly-Polarized Pulse Light

In PR-SHG-M, while the polarization angle of a linearly-polarized laser light is rotated, the corresponding SHG images, namely polarization-resolved SHG images, are acquired [9]–[12]. When its polarization angle is rotated before propagating in the LMA-PCF as shown in Fig. 1(a), the LMA-PCF has to maintain the same polarization condition during the propagation. We first evaluated the polarization characteristics of the laser light before and after propagating in a 75-cm LMA-PCF with a curvature radius of 7.5 cm when the vertically linear-polarized laser light is incident into the LMA-PCF. To this end, we placed an additional analyzer before or after the LMA-PCF [not shown in Fig. 1(a)] and analyzed the polarization characteristics by rotating the analyzer at a step of 20 degree. Fig. 2 shows a comparison of polarization characteristics (a) before and (b) after propagating in the LMA-PCF, which are illustrated as a radar graph of the optical intensity with respect to the polarization angle. In this radar graph, the major axis gives the dominant polarization direction, and a ratio of the minor axis to the major axis is corresponding to the extinction ratio. For example, a figure-of-eight profile indicates the linear polarization whereas a circular profile is given by the circular polarization or completely random polarization. Since the similar figure-of-eight profile was confirmed in Fig. 2(a) and 2(b), the linearly polarized light was maintained during the propagation of the LMA-PCF. Even though the LMA-PCF used is not a polarization-maintained fiber, such polarization-maintaining capability is an interesting profile in the LMA-PCF.

We next evaluated the polarization characteristics of the laser light after propagating in the LMA-PCF when the linear-polarization angle of the incident laser light is rotated

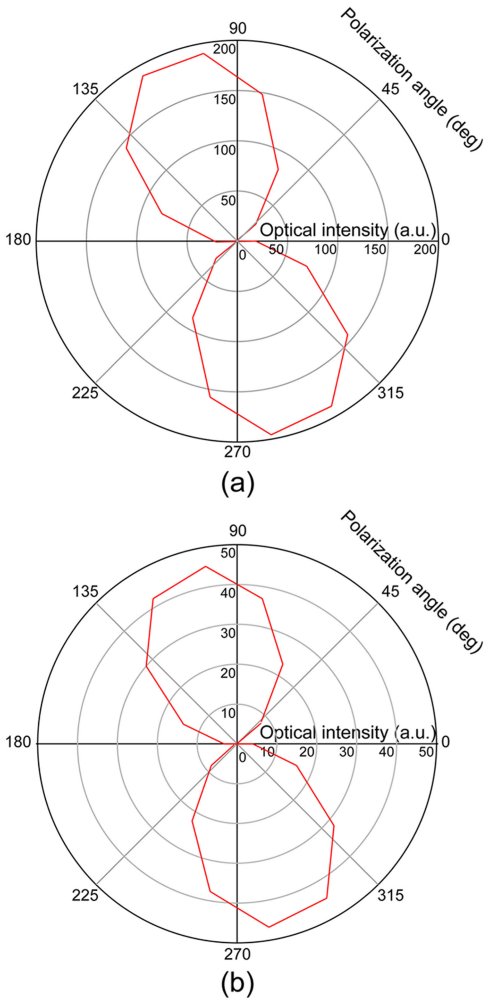

Fig. 2. Comparison of polarization characteristics (a) before propagating in the LMA-PCF and (b) after propagating in the LMA-PCF with a curvature radius of 7.5 cm.

by $\lambda/2$. Fig. 3(a) shows a relation of the dominant polarization direction between the incident light and the output light from the LMA-PCF. A good linear relation was confirmed between them. On the other hand, Fig. 3(b) shows the extinction ratio with respect to the linear-polarization angle of the incident laser light. The extinction ratio largely changed depending on the linear-polarization angle. One possible reason for such change is in bending of the LMA-PCF with a curvature radius of 7.5 cm; however, it is not clear at the present stage. Such dependence has to be compensated for precise polarization-resolved SHG imaging.

B. Ex Vivo Polarization-Resolved SHG Imaging of Sliced Tendon Specimen With Uniaxial Collagen Fiber Orientation

We next performed *ex vivo* polarization-resolved SHG imaging of a sliced tendon specimen by the constructed hand-held PR-SHG-M setup. To obtain a spatial distribution of collagen fiber orientation in the dermis, orthogonally polarization-resolved SHG imaging was applied for the samples. Polarization anisotropy of SHG light (α) was defined using the following

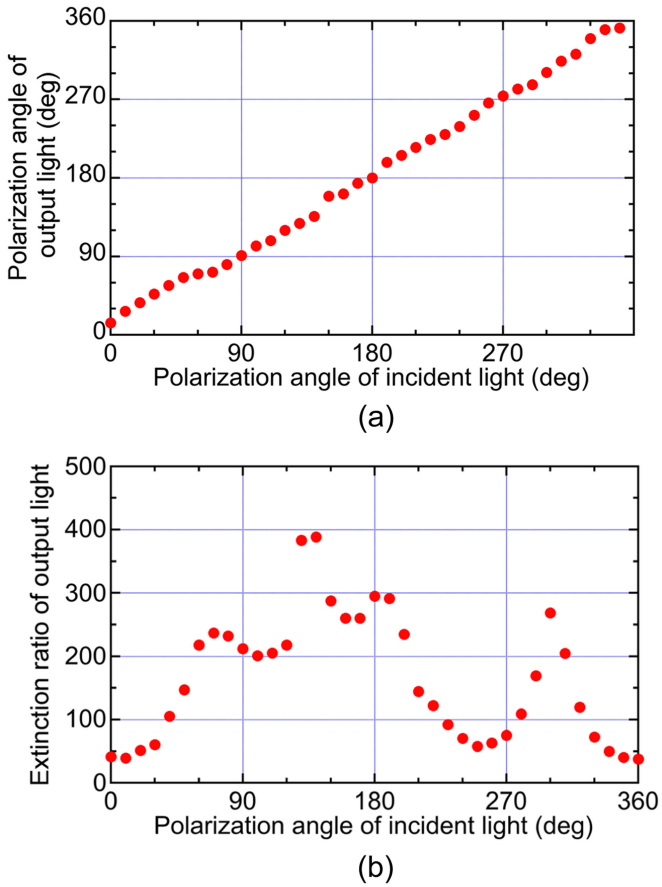

Fig. 3. (a) Relation of the dominant polarization direction between the incident light and the output light from the LMA-PCF. (b) Extinction ratio of the output light with respect to the linear-polarization angle of the incident laser light.

equation [23], [24]

$$\alpha = \frac{I_V - I_H}{I_V + I_H} \tag{1}$$

where I_V and I_H are SHG intensities when the incident light is vertically and horizontally polarized, respectively. Then the α image was calculated by substituting I_V and I_H values at each pixel of two orthogonally polarization-resolved SHG images for Eq. (1). Collagen fiber orientation is uniaxial for $\alpha = \pm 1$ and random or biaxial for $\alpha = 0$. The sign of α value provides the dominant direction of the collagen fiber orientation: positive for a vertical orientation (blue) and negative for a horizontal orientation (red). Fig. 4 shows (a) I_H image, (b) I_V image, and (c) α image (image size = 400 μm by 400 μm, pixel size = 256 pixels by 256 pixels) when the collagen fiber orientation of the sample was directed at horizontal direction. Due to the polarization dependence of SHG light efficiency, there is a small difference of image brightness between Fig. 4(a) and 4(b), leading to the reddish α image. On the other hand, Fig. 5 shows (a) I_H image, (b) I_V image, and (c) α image when the collagen fiber orientation of the sample was directed at the vertical direction. In this case, I_H image was darker than I_V image, and hence the α image became bluish. Such the reddish α image in Fig. 4(c) and the bluish α image in Fig. 5(c) correctly reflected the collagen fiber orientation of the tendon specimen. In this way, we confirmed

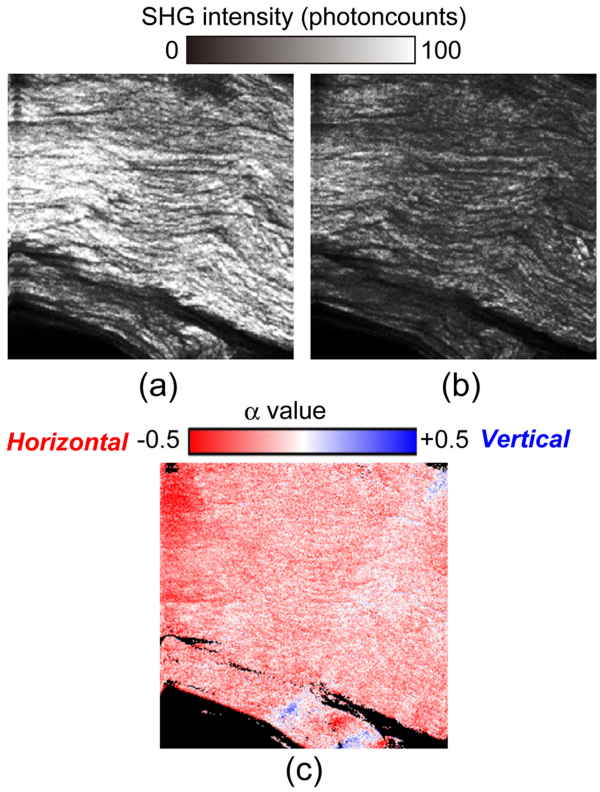

Fig. 4. (a) I_H image, (b) I_V image, and (c) α image when the collagen orientation of the sample was directed at the horizontal direction. Image size is 400 μm by 400 μm, corresponding to pixel size of 256 pixels by 256 pixels.

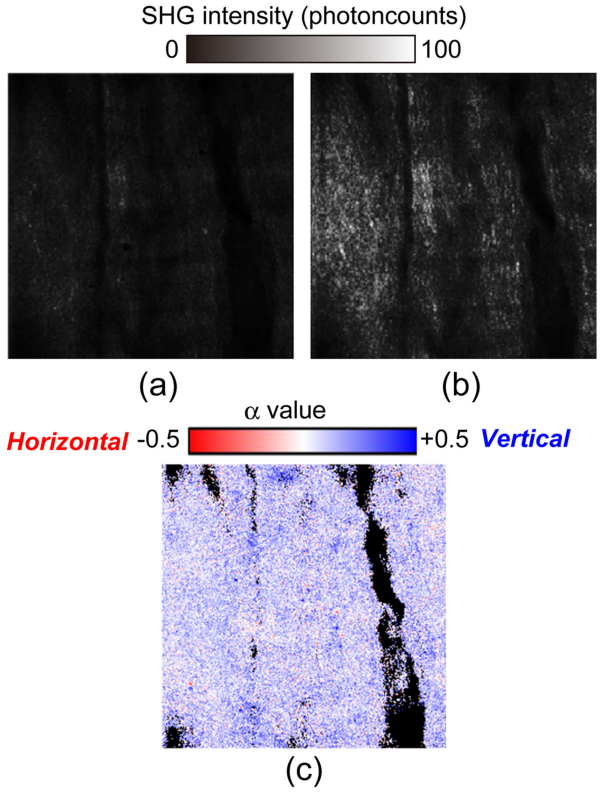

Fig. 5. (a) I_H image, (b) I_V image, and (c) α image when the collagen orientation of the sample was directed at the vertical direction. Image size is 400 μm by 400 μm, corresponding to pixel size of 256 pixels by 256 pixels.

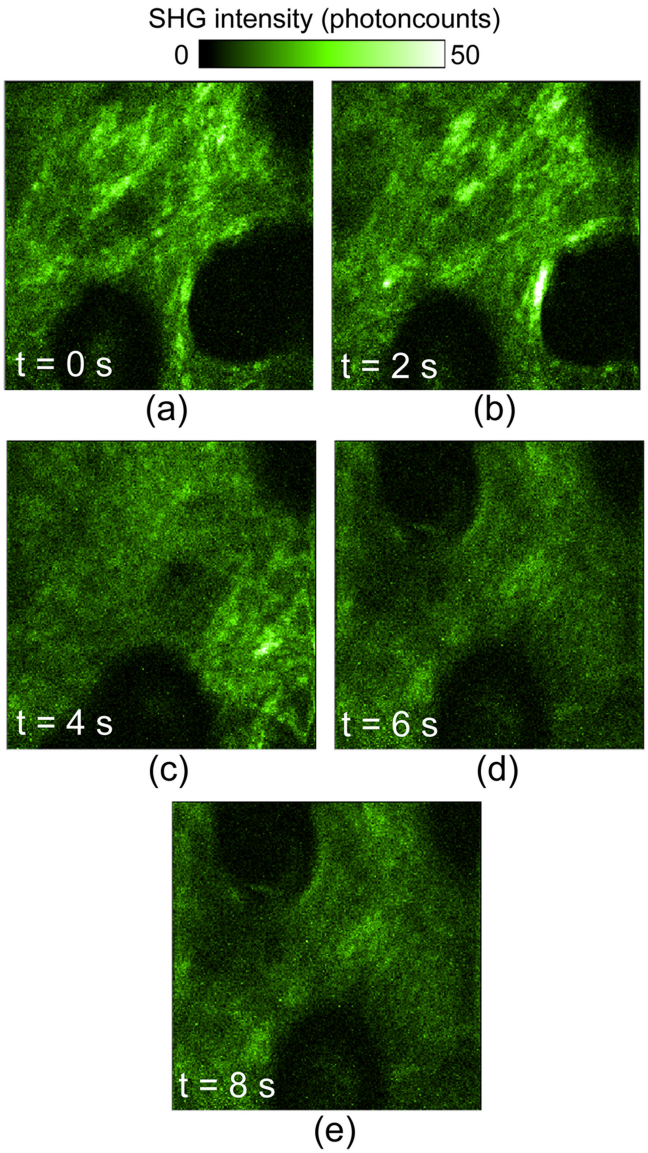

Fig. 6. A series of SHG images of dermal collagen fibers in human cheek skin acquired at a rate of 0.5 image/s. (a) t = 0 s, (b) t = 2 s, (c) t = 4 s, (d) t = 6 s, and (e) t = 8 s. Image size is 400 μm by 400 μm, corresponding to pixel size of 256 pixels by 256 pixels.

the effectiveness of the constructed hand-held PR-SHG-M setup for evaluation of collagen fiber orientation.

C. In Vivo SHG Imaging of Dermal Collagen Fibers in Human Cheek Skin

We performed *in vivo* SHG imaging of dermal collagen fibers in human cheek skin by the constructed hand-held PR-SHG-M. Since the cheek skin does not have outstanding features in the collagen fiber orientation [24], we acquired several SHG images, in place of polarization-resolved SHG images, at a measurement rate of 0.5 image/s to demonstrate its *in vivo* SHG imaging capability of dermal collagen fibers in human skin. Fig. 6 shows a series of SHG images at an interval of 2 s (image size = 400 μm by 400 μm, pixel size = 256 pixels by 256 pixels). The obtained image quality and contrast were similar to those in the bulky

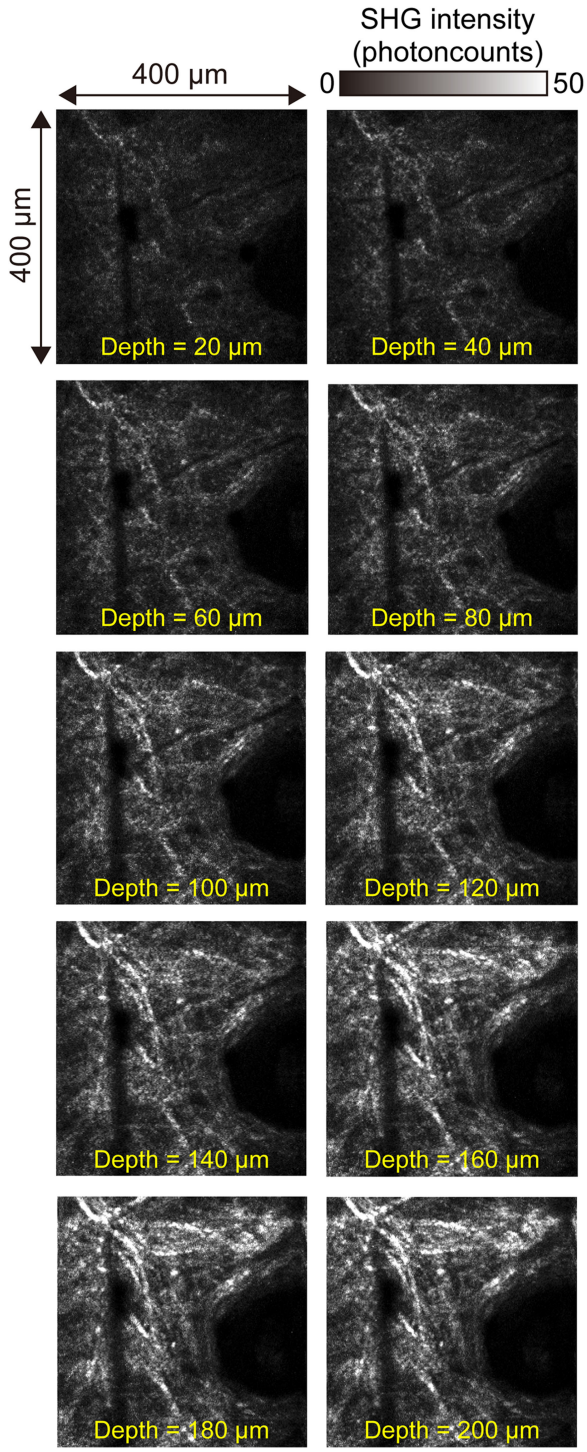

Fig. 7. Result of *in vivo* depth-resolved SHG imaging of dermal collagen fibers in human cheek skin.

SHG-M in the previous study [18], [19], [24]. Although motion artefact was confirmed in them due to the slow imaging rate, the detailed distribution of collagen fibers was clearly confirmed. This means that it is possible to perform quantitative analysis of collagen fiber structure based on SHG image analysis with the hand-held SHG-M [19], [28].

Dermal collagen fibers significantly change their structure depending on the depth while SHG-M has the intrinsic depth

selectivity. To confirm such features, we demonstrated the *in vivo* depth-resolved SHG imaging of dermal collagen fibers in human cheek skin by scanning the hand-held PR-SHG-M probe along the depth direction. Fig. 7 shows a series of *in vivo* depth-resolved SHG images acquired at a step of 20 μm for dermal collagen fibers in human cheek skin (image size = 1.6 mm by 1.6 mm corresponding to 256 pixels by 256 pixels, image acquisition time $\approx$ 20 s). We here defined the skin surface to be 0 μm in depth. These SHG images clearly indicated the depth dependence of dermal collagen fiber structure: thin collagen fibers distributed at the upper dermis corresponding to the papillary dermis whereas thick collagen fibers were observed in the lower dermis corresponding to the reticular dermis. These findings are in good agreement with our previous researches using the bulky SHG-M [18], [19]. The maximum probing depth of the present SHG-M is limited by the working distance of the OL (=350 μm) and a thickness ($\sim$100 μm) of a thin glass plate between the OL and the sample surface, rather than the vanished SHG light. Use of a longer working distance, high-NA OL will increase the penetration depth beyond 200 μm.

IV. Conclusion

We constructed the fiber-coupled, hand-held PR-SHG-M by use of the 1250-nm Cr:Forsterite laser, the 75-cm LMA-PCF, and the hand-held probe. The LMA-PCF could deliver the ultrashort pulse light without the significant change of its linear polarization as well as its pulse duration [27]. Also, the effectiveness of the fiber-coupled, hand-held PR-SHG-M was confirmed in the *ex-vivo* polarization-resolved SHG imaging of the sliced tendon specimen. Finally, we demonstrated *in vivo* SHG imaging of dermal collagen fibers in human cheek skin. The image quality and contrast in the hand-held PR-SHG-M are comparable to those in the bulky SHG-M. Also, use of the long LMA-PCF largely increases the flexibility of the hand-held SHG-M for practical applications. Although the Cr:Forsterite laser is still bulky for clinical application, use of a mode-locked fiber laser [29] or mode-locked integrated external-cavity surface emitting laser (MIXSEL) [30] is an alternative compact laser source at this wavelength band. The fiber-coupled, hand-held PR-SHG-M will be open the door for *in vivo* dermatological applications in hospital as well as time-series monitoring of collagen fiber production by cells cultured in an incubator [8] and *in vivo* observation of the histological and mechanical features of tendon healing [31].

Acknowledgment

The authors would like to acknowledge Ms. Shoko Lewis of Tokushima University, Japan, for her help in the preparation of the manuscript.

References

[1] P. J. Campagnola and C.-Y. Dong, "Second harmonic generation microscopy: Principles and applications to disease diagnosis," *Laser Photon. Rev.*, vol. 5, pp. 13–26, Dec. 2011.

[2] K. Lu *et al.*, "Multiphoton laser scanning microscopy of localized scleroderma," *Skin Res. Technol.*, vol. 15, pp. 489–495, Nov. 2009.

[3] R. Cicchi *et al.*, "Scoring of collagen organization in healthy and diseased human dermis by multiphoton microscopy," *J. Biophoton.*, vol. 3, pp. 34–43, Jan. 2010.

[4] M. Han, G. Giese, and J. F. Bille, "Second harmonic generation imaging of collagen fibrils in cornea and sclera," *Opt. Express*, vol. 13, pp. 5791–5797, Jul. 2005.

[5] R. Ambekar, M. Chittenden, I. Jasiuk, and K. C. Toussaint, Jr., "Quantitative second-harmonic generation microscopy for imaging porcine cortical bone: Comparison to SEM and its potential to investigate age-related changes," *Bone*, vol. 50, pp. 643–650, Mar. 2012.

[6] J. C. Mansfield, C. P. Winlove, J. Moger, and S. J. Matcher, "Collagen fiber arrangement in normal and dis-eased cartilage studied by polarization sensitive nonlinear microscopy," *J. Biomed. Opt.*, vol. 13, Jul./Aug. 2008, Art. no. 044020.

[7] C.-Y. Park *et al.*, "Revisiting ciliary muscle tendons and their connections with the trabecular meshwork by two photon excitation microscopic imaging," *Investigative Ophthalmol. Vis. Sci.*, vol. 57, pp. 1096–1105, Mar. 2016.

[8] E. Hase, O. Matsubara, T. Minamikawa, K. Sato, and T. Yasui, "*In situ* time-series monitoring of collagen fibers produced by standing-cultured osteoblasts using a second-harmonic-generation microscope," *Appl. Opt.*, vol. 55, pp. 3261–3267, Apr. 2016.

[9] P. C. Stoller, B.-M. Kim, A. M. Rubenchik, K. M. Reiser, and L. B. Da Silva, "Polarization-dependent optical second-harmonic imaging of rat-tail tendon," *J. Biomed. Opt.*, vol. 7, pp. 205–215, Apr. 2002.

[10] P. Stoller, K. M. Reiser, P. M. Celliers, and A. M. Rubenchik, "Polarization-modulated second harmonic generation in collagen," *Biophys. J.*, vol. 82, pp. 3330–3342, Jun. 2002.

[11] T. Yasui, Y. Tohno, and T. Araki, "Determination of collagen fiber orientation in human tissue by polarization measurement of molecular second-harmonic-generation light," *Appl. Opt.*, vol. 43, pp. 2861–2867, May 2004.

[12] T. Yasui, Y. Tohno, and T. Araki, "Characterization of collagen orientation in human dermis by two-dimensional second-harmonic-generation polarimetry," *J. Biomed. Opt.*, vol. 9, pp. 259–264, Mar./Apr. 2004.

[13] H. Bao, A. Boussioutas, R. Jeremy, S. Russell, and M. Gu, "Second harmonic generation imaging via nonlinear endomicroscopy," *Opt. Express*, vol. 18, pp. 1255–1260, Jan. 2010.

[14] Á. Krolopp *et al.*, "Handheld nonlinear microscope system comprising a 2 MHz repetition rate, mode-locked Yb-fiber laser for in vivo biomedical imaging," *Biomed. Opt. Express*, vol. 7, pp. 3531–3542, Sep. 2016.

[15] I.-H. Chen, S.-W. Chu, C.-K. Sun, P.-C. Cheng, and B.-L. Lin, "Wavelength dependent damage in biological multi-photon confocal microscopy: A micro-spectroscopic comparison between femtosecond Ti:sapphire and Cr:forsterite laser sources," *Opt. Quantum Electron.*, vol. 34, pp. 1251–1266, Dec. 2002.

[16] S.-W. Chu *et al.*, "*In vivo* developmental biology study using noninvasive multi-harmonic generation microscopy," *Opt. Express*, vol. 11, pp. 3093–3099, Nov. 2003.

[17] S.-P. Tai *et al.*, "*In vivo* optical biopsy of hamster oral cavity with epi-third-harmonic-generation microscopy," *Opt. Express*, vol. 14, pp. 6178–6187, Jun. 2006.

[18] T. Yasui, Y. Takahashi, M. Ito, S. Fukushima, and T. Araki, "*Ex vivo* and *in vivo* second-harmonic-generation imaging of dermal collagen fiber in skin: Comparison of imaging characteristics between mode-locked Cr:Forsterite and Ti:Sapphire lasers," *Appl. Opt.*, vol. 48, pp. D88–D95, Apr. 2009.

[19] T. Yasui *et al.*, "*In vivo* observation of age-related structural changes of dermal collagen in human facial skin using collagen-sensitive second harmonic generation microscope equipped with 1250-nm mode-locked Cr:Forsterite laser," *J. Biomed. Opt.*, vol. 18, Mar. 2013, Art. no. 031108.

[20] R. Tanaka *et al.*, "*In vivo* visualization of dermal collagen fiber in skin burn by collagen-sensitive second-harmonic-generation microscopy," *J. Biomed. Opt.*, vol. 18, Jun. 2013, Art. no. 061231.

[21] T. Yasui, R. Tanaka, E. Hase, S. Fukushima, and T. Araki, "*In vivo* time-lapse imaging of skin burn wound healing using second-harmonic generation microscopy," *Proc. SPIE*, vol. 8948, Feb. 2014, Art. no. 89480B.

[22] G. Deka, W.-W. Wu, and F.-J. Kao, "*In vivo* wound healing diagnosis with second harmonic and fluorescence lifetime imaging," *J. Biomed. Opt.*, vol. 18, Dec. 2012, Art. no. 061222.

[23] T. Yasui *et al.*, "Observation of dermal collagen fiber in wrinkled skin using polarization-resolved second-harmonic-generation microscopy," *Opt. Express*, vol. 17, pp. 912–923, Jan. 2009.

[24] Y. Tanaka *et al.*, "Motion-artifact-robust, polarization-resolved second-harmonic-generation microscopy based on rapid polarization switching with electro-optic Pockells cell and its application to *in vivo* visualization of collagen fiber orientation in human facial skin," *Biomed. Opt. Express*, vol. 5, pp. 1099–1113, Apr. 2014.

[25] J. C. Knight, T. A. Birks, R. F. Cregan, P. S. J. Russell, and P. D. de Sandro, "Large mode area photonic crystal fibre," *Electron. Lett.*, vol. 34, pp. 1347–1348, Jun. 1998.
[26] S.-H. Chia *et al.*, "Miniaturized video-rate epi-third-harmonic-generation fiber-microscope," *Opt. Express*, vol. 18, pp. 17382–17391, Aug. 2010.
[27] K. Atsuta, Y. Ogura, E. Hase, T. Minamikawa, and T. Yasui, "*In situ* monitoring of collagen fibers in human skin using a photonic-crystal-fiber-coupled, hand-held, second-harmonic-generation microscope," *Proc. SPIE*, vol. 10069, Feb. 2017, Art. no. 100692B.
[28] Y. Ogura, Y. Tanaka, E. Hase, T. Yamashita, and T. Yasui, "Texture analysis of second-harmonic-generation images for quantitative analysis of reticular dermal collagen fiber *in vivo* in human facial cheek skin," *Exp. Dermatol.*, online published, doi: 10.1111/exd.13560.
[29] W. Liu *et al.*, "Energetic ultrafast fiber laser sources tunable in 1030–1215 nm for deep tissue multi-photon microscopy," *Opt. Express*, vol. 25, pp. 6822–6831, Mar. 2017.
[30] A. R. Bellancourt *et al.*, "Modelocked integrated external-cavity surface emitting laser (MIXSEL)," *IET Optoelectron.*, vol. 3, pp. 61–72, Apr. 2009.
[31] E. Hase *et al.*, "Evaluation of the histological and mechanical features of tendon healing in a rabbit model with the use of second-harmonic-generation imaging and tensile testing," *Bone Joint Res.*, vol. 5, pp. 577–585, Nov. 2016.

Yuki Ogura received the master's degree in engineering from Osaka University, Suita, Japan, in 2001. She is currently working toward the Ph.D. degree with Tokushima University, Tokushima, Japan.

Since 2001, she has been with the Shiseido Research Center, Yokohama, Japan. Her research interests include skin measurements and second-harmonic-generation microscopy.

Kosuke Atsuta received the master's degree in engineering from Tokushima University, Tokushima, Japan, in 2016.

Since 2016, he has been with the Seiko Epson Corp., Suwa, Japan. His current research focuses on second-harmonic-generation microscopy.

Eiji Hase was born in Tokushima, Japan, in 1989. He received the B.S., M.S., and Ph.D. degrees in engineering from Tokushima University, Tokushima, Japan, in 2012, 2014, and 2017, respectively.

From 2014 to 2017, he was a Research Associate with the JST, ERATO, Minoshima Intelligent Optical Synthesizer Project. Since 2017, he has been a Research Scientist with the Research and Utilization Division, Japan Synchrotron Radiation Research Institute, Sayo, Japan, and a Visiting Associate Professor with the Graduate School of Technology, Industrial and Social Sciences, Tokushima University. His research interests include biomedical imaging and biomechanical analysis using femtosecond laser and synchrotron X-ray.

Dr. Hase was the recipient of the Optical Society of Japan Best Presentation Award in 2016, the Japanese Society for Medical and Biological Engineering Symposium Award in 2016, and SPIE BiOS2016 in Photonics West 2016 Student Poster Awards in 2016.

Takeo Minamikawa was born in Ibraki, Japan, in 1983. He received the B.S., M.S., and Ph.D. degrees in engineering from Osaka University, Osaka, Japan, in 2006, 2008, and 2010, respectively.

From 2010 to 2013, he was a Research Fellowship for Young Scientists with the Japan Society for the Promotion of Science. From 2013 to 2015, he was an Assistant Professor with the Department of Pathology and Cell Regulation, Graduate School of Medical Science, Kyoto Prefectural University of Medicine. Since 2015, he has been an Associate Professor with the Department of Mechanical Science, Division of Science and Technology, Graduate School of Technology, Industrial and Social Sciences, Tokushima University, Tokushima, Japan. He is the author of two book chapters, more than 30 articles, and more than 15 inventions. His research interests include Raman microspectroscopy and optical frequency comb. He holds three patents.

Dr. Minamikawa was the recipient of the Japan Society for Precision Engineering Best Presentation Award in 2016, the Japanese Society of Pathology Poster Presentation Award in 2015, and the Funai Foundation for Information Technology Research Award in 2011.

Takeshi Yasui received the first Ph.D. degree in engineering from the University of Tokushima, Tokushima, Japan, in 1997, and the second Ph.D. degree in medical science from the Nara Medical University, Yagi, Japan, in 2013.

From 1997 to 1999, he was a Postdoctoral Research Fellow with the National Research Laboratory of Metrology, Japan. He was with the Graduate School of Engineering Science, Osaka University from 1999 to 2010, and was briefly with the University of Bordeaux I in 2007 and 2012, and with the University of Littoral Côte d'Opale in 2010 as an Invited Professor. He is currently a Professor with the Graduate School of Technology, Industrial and Social Sciences, Tokushima University, Tokushima, Japan, has been the Vice Director of Research Support with the same university since 2016, and an Invited Professor with the Graduate School of Engineering Science, Osaka University, Toyonaka, Japan. His research interests include THz instrumentation and metrology, second-harmonic-generation microscopy, and optical frequency comb.

Prof. Yasui is a member of the Optical Society of America, the International Society for Optical Engineering, the Japan Society of Applied Physics, the Optical Society of Japan, the Laser Society of Japan, the Japanese Society for Medical and Biological Engineering, and the Japan Society of Mechanical Engineers. He was the recipient of the Award for the Most Promising Young Scientist from the Optical Society of Japan in 1998, the Sakamoto Award from the Japan Society of Medical Electronics and Biological Engineering in 2006, the Optics Paper Award from the Japan Society of Applied Physics, the Funai Award from the Japan Society of Mechanical Engineers in 2009, and the Original Paper Award from the Laser Society of Japan in 2013.